

MIXING ALONG THE RED GIANT BRANCH IN METAL-POOR FIELD STARS

E. CARRETTA¹ AND R.G. GRATTON¹

*Osservatorio Astronomico di Padova
Vicolo dell'Osservatorio 5, I-35122 Padova, ITALY*

C. SNEDEN²

*Department of Astronomy and McDonald Observatory
The University of Texas at Austin, USA*

AND

A. BRAGAGLIA³

*Osservatorio Astronomico di Bologna
via Ranzani 1, I-40127 Bologna, ITALY*

1. Introduction

Stellar models predict that as a small mass star evolves up the RGB, the outer convective envelope expands inward and penetrates into the CN-cycle processed interior regions (*first dredge-up*). Approximately, the outer 50% of the star by mass is involved in this mixing that brings to the surface mainly ^{13}C and ^{14}N , while the primordial ^{12}C and fragile, light elements like Li, Be, and B are transported from the surface to the interior. Results for old disk field giants (Shetrone et al. 1993) and metal-poor stars (Sneden et al. 1986) show that the first dredge-up occurs at the predicted luminosities; however, mixing in bright giants is much more extreme than predicted by evolutionary models.

On the other side, some further mixing is possible in the latest phases of the RGB (see e.g., Charbonnel 1994, 1995): in fact, after the end of the dredge-up phase is reached, the convective envelope begins to recede, leaving behind a chemical discontinuity. This is subsequently contacted by the H-burning shell, giving rise to the so-called RGB bump. Before this contact is made, the H-burning shell is advancing through a region where there are appreciable composition gradients, which should inhibit any (rotational induced) mixing. Thereafter, since there is no mean molecular

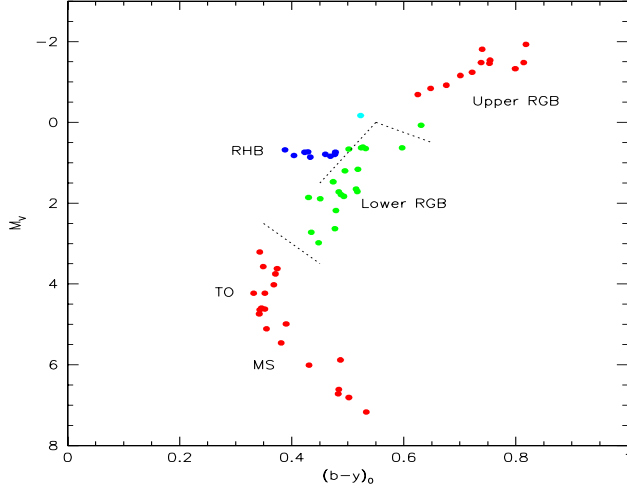


Figure 1. Selected sample: we define as lower red giant branch (lower-RGB) the evolutionary phase between first dredge-up completion and the RGB bump: small mass stars on the lower-RGB should have a well defined set of CNO and Li abundances, distinct from that observed in main sequence stars (MS stars, which have not yet experienced the first dredge up) and upper-RGB stars (hereinafter, upper-RGB stars are those stars first ascending the red giant branch, which are brighter than the RGB bump).

weight gradient between the convective envelope and the near vicinity of the shell, it is possible that circulation currents, perhaps driven by meridional circulations activated by core rotation (Sweigart & Mengel 1979) give rise to further mixing.

In principle, globular clusters offer a unique opportunity to verify this scheme, since they provide a large number of stars located at the same distance (thus allowing an accurate definition of the evolutionary status of individual stars), having the same age (thus similar masses evolving along the RGB), and, hopefully, the same initial chemical composition. However, surface abundances of globular cluster RGB stars have revealed a complex phenomenology (for a summary, see Kraft 1994), that has defied insofar any attempt of a detailed explanation. This is likely due to the fact that the surface abundances of these stars are significantly affected by several major factors: deep mixing within individual stars, primordial inhomogeneities within a cluster, and perhaps accretion of nuclearly processed material during the early phases of the cluster evolution. Furthermore, it is becoming increasingly clear that the dense environment plays an important role on determining other basic cluster features (like the colour of the horizontal branch), either by causing systematic variations in the basic stellar properties (like e.g., the initial angular momentum), or in favouring pollution of

the surface layers of stars by ejecta from other stars, or both.

To solve these issues, it is necessary to first understand the evolution of single undisturbed small mass stars in the field, in a restricted range of mass and metal abundance (both of them affecting the luminosity of the RGB bump).

2. Sample selection and observations

To this purpose, we selected a sample from Anthony-Twarog & Twarog (1994, ATT) for the evolved stars) and Schuster & Nissen (1989) for the main sequence and turn-off stars, plus a few local subdwarfs from Clementini et al. (1998). We restricted to metallicities in the range $-2 < [\text{Fe}/\text{H}] < -1$, in order to: (i) avoid possible massive interlopers (thin disk stars), (ii) have a large number of moderately bright stars with accurate absolute magnitudes, hence clear evolutionary phases, and (iii) avoid complications from large star-to-star abundance variations present among the most metal-poor stars.

The resulting sample (62 stars) is shown in Figure 1; evolutionary phases are derived from the position on the $(b - y)_0 - c_{10}$ and the calassical colour magnitude diagram; M_V values are from ATT (giants and subgiants) or from Hipparcos (dwarfs).

High S/N (> 100), high resolution ($R > 50,000$) spectra were acquired at the McDonald Observatory (2.7m telescope + “2d-coudé” echelle spectrometer, spectral range $3800 \leq \lambda \leq 9000 \text{ \AA}$) and at ESO (CAT+CES spectrograph, spectral regions centered at 4230, 4380, 5680, 6300, 6700, and 7780 \AA), to measure abundance indicators for Li, C, N, O, Na and Fe.

3. Atmospheric parameters and abundance analysis

Effective temperatures (T_{eff} ’s) were derived from the dereddened $(B - V)_0$ and $(b - y)_0$ colours using colour- T_{eff} transformations from Kurucz (1995) models with no overshooting, and reddening from ATT or Carretta, Gratton & Sneden (1999). Note that no empirical correction was required for these calibrations (see e.g., Castelli, Gratton & Kurucz 1997). Gravities were derived from absolute magnitudes and T_{eff} ’s, assuming a mass $M = 0.85 M_{\odot}$ for all stars and B.C.’s from Kurucz (1995). Eliminating trends of abundances derived from Fe I lines versus EWs for stars with McDonald spectra, we obtained microturbulent velocities v_t ’s for this subsample and a tight relation $v_t = f(T_{\text{eff}}, \log g)$. This was used to derive accurate v_t values for stars with CAT spectra (having very few Fe lines measured).

The abundance analysis was performed using Kurucz (1995) model atmospheres with no overshooting. Further details are in Gratton et al. (2000).

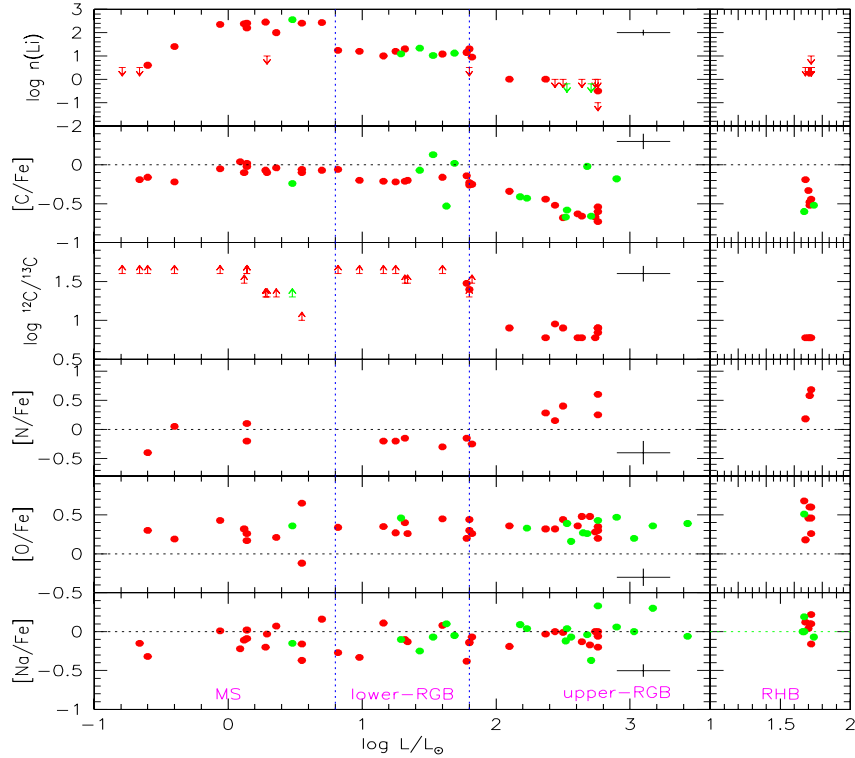


Figure 2. Run of the abundance of Li, of the abundance ratios [C/Fe], [N/Fe], [O/Fe] and [Na/Fe], and of the isotopic ratio $^{12}\text{C}/^{13}\text{C}$ with luminosity for stars with $-2 < [\text{Fe}/\text{H}] < -1$. Filled symbols are actual measures; arrows are upper (for Li) or lower (for $^{12}\text{C}/^{13}\text{C}$) limits. Typical error bars for the various quantities are shown. Dashed lines separate various evolutionary phases. Results for red HB (RHB) stars are plotted separately for clarity.

Abundances for Fe I, Fe II, O I, Na I, α -elements and heavy elements were derived from measured equivalent widths (EWs). Whenever possible, we complemented the rather few atomic lines measured on CAT spectra with lists of accurate (errors ≤ 3 mÅ) and homogeneous EWs from literature (see Gratton, Carretta & Castelli 1997 for references).

O abundances were obtained from both forbidden and permitted lines. Abundances from these last (as well as the Na abundances from the 5682-88 Å and 6154-60 Å doublets) include corrections for departures from LTE (Gratton et al. 1999). Average [O/Fe] ratios were computed after a small offset of 0.08 dex between the abundances from [O I] and O I lines was accounted for.

C abundances as well $^{12}\text{C}/^{13}\text{C}$ isotopic ratios were derived from spectral synthesis of the G-band around 4300 Å. Synthetic spectra computations of

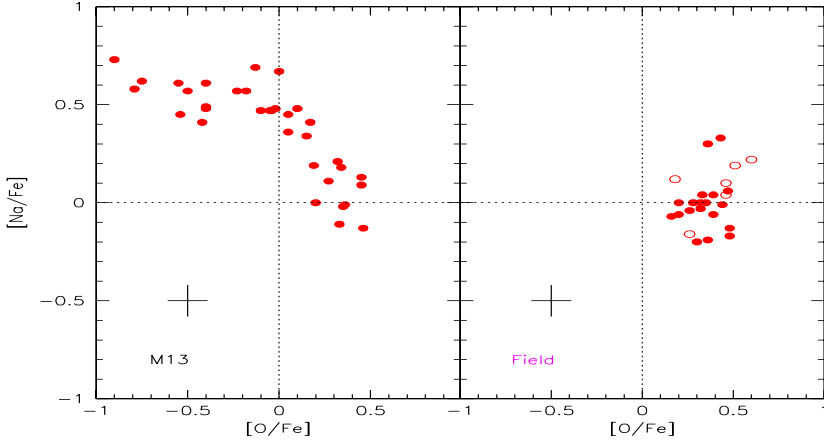


Figure 3. The Na-O anticorrelation for field stars and for stars in M13. Filled symbols are stars first ascending the RGB (only upper-RGB stars are shown); open symbols are RHB stars. Error bars are shown at the bottom left.

the (0,0) and (1,1) bandheads of the violet band of CN were used to derive N abundances for the 24 program stars with McDonald spectra.

Li abundances have been derived from comparison to synthetic spectra, and complemented with data from Pilachowski, Sneden & Booth (1993, PSB), after Fe and Li abundances from their analysis were increased to compensate the offsets (0.09 and 0.21 dex, respectively) with respect to our results, due to our higher T_{eff} 's (112 ± 32 K, from 14 stars in common with PSB).

4. Results

Results for Li, C, N, O, Na and $^{12}\text{C}/^{13}\text{C}$ isotopic ratios are summarized in Figure 2 for the 62 program stars with accurate evolutionary phase, plus 43 stars more having accurate abundances for some of these elements and similarly well defined luminosities from the literature. From Figure 2 we can see that small mass lower-RGB stars (i.e., stars brighter than the first dredge-up luminosity and fainter than the RGB bump) have abundances of light elements in agreement with predictions from classical evolutionary models: only marginal changes occur for CNO elements, while dilution within the convective envelope causes the surface Li abundance to decrease by a factor of ~ 20 .

A second, distinct mixing episode occurs in most (perhaps all) small mass metal-poor stars just after the RGB bump, when the molecular weight barrier left by the maximum inward penetration of the convective shell is canceled by the outward expansion of the H-burning shell, in agreement

with recent theoretical predictions.

In field stars, this second mixing episode only reaches regions of incomplete CNO burning: it causes a depletion of the surface ^{12}C abundance by about a factor of 2.5, and a corresponding increase in the N abundance by about a factor of 4. The $^{12}\text{C}/^{13}\text{C}$ is lowered to about 6 to 10 (close to, but distinctly larger than the equilibrium value of 3.5), while practically all remaining Li is burnt.

However, an O-Na anti-correlation such as typically observed among globular cluster stars (see Figure 3) is not present in field stars. None of the 29 field stars more evolved than the RGB bump (including 8 RHB stars) shows any sign of O depletion or Na enhancement. This means that in field stars the second mixing episode is not deep enough to reach regions where ON-burning occurs.

References

1. Anthony-Twarog, B.J., Twarog, B.A. (1994) Reddening estimation for halo red giants using uvby photometry, *Astron. J.* **107**, 1577
2. Carretta, E., Gratton, R.G., Sneden, C. (1999), submitted to *Astron. Astrophys*
3. Castelli, F., Gratton, R.G., Kurucz, R.L. (1997), Notes on the convection in the ATLAS9 model atmospheres, *Astron. Astrophys* **318**, 841
4. Charbonnel, C. (1994), Clues for non-standard mixing on the red giant branch from C-12/C-13 and C-12/N-14 ratios in evolved star, *Astron. Astrophys* **282**, 811
5. Charbonnel, C. (1995) A Consistent Explanation for $^{12}\text{C}/^{13}\text{C}$, ^{7}Li and ^{3}He Anomalies in Red Giant Stars *Ap. J.* **453**, L41
6. Clementini, G., Gratton, R.G., Carretta, E., Sneden, C. (1998) Homogeneous photometry and metal abundances for a large sample of Hipparcos metal-poor stars, *Mon. Not. R. Astr. Soc* **302**, 22
7. Gratton, R.G., Carretta, E., Castelli, F. (1997) Abundances of light elements in metal-poor stars. I. Atmospheric parameters and a new Teff scale, *Astron. Astrophys.* **314**, 191
8. Gratton, R.G., Gustafsson, B., Carretta, E., Eriksson, K. (1999) Abundances of light elements in metal-poor stars. II. Non-LTE abundance corrections *Astron. Astrophys.*, **350**, 955
9. Gratton, R.G., Sneden, C., Carretta, E., Bragaglia, A. 2000, *Astron. Astrophys.*, in press
10. Kraft, R.P. (1994) Abundance differences among globular-cluster giants: Primordial versus evolutionary scenarios, *Pub. Astr. Soc. Pacific* **106**, 553
11. Kurucz, R.L. (1995), CD-ROM 13
12. Pilachowski, C.A., Sneden, C., Booth, J. (1993) The abundance of lithium in metal-poor subgiant stars, *Ap. J.* **407**, 699
13. Schuster, W.J., Nissen, P.E. (1989) uvby-beta photometry of high-velocity and metal-poor stars. III - Metallicities and ages of the halo star, *Astron. Astrophys.* **222**, 69
14. Shetrone, M.D., Sneden, C., Pilachowski, C.A. (1993) Carbon isotope ratios and lithium abundances in old disk giants, *Pub. Astr. Soc. Pacific* **105**, 337
15. Sneden, C., Pilachowski, C.A., VandenBerg, D.A. (1986) Carbon isotope ratios in field Population II giant star, *Ap. J.* **311**, 826
16. Sweigart, A.V., Mengel, J.G. (1979) Meridional circulation and CNO anomalies in red giant stars, *Ap. J.* **229**, 624